

Research on the Quality of Heterogeneous Welded Joints Between Copper and Stainless

OANA-ROXANA CHIVU*, CORNELIU RONTESCU, DUMITRU-TITI CICIC

University Politehnica of Bucharest, Department of Materials Technology and Welding, 202 Splaiul Independentei, 060021, Bucharest, Romania

In the present paper, a series of experimental results on the quality of connections between heterogeneous copper and stainless steel are presented, using the methods of optical microscopic, scanning electron microscopy (SEM) and the spectroscopy method of X-ray energy dispersion. The welded joints were made by using the process of welding in protective gas environment with non-fusible electrode (GTAW). Electronic and optical microscopic analysis have discovered that there were no cracks in welded joint area leading to the loss of physical and mechanical properties thereof. There is also a good mixing of molten metal through the diffusion of copper into the matrix of the stainless steel in the crossing area.

Keywords: cooper, stainless steel, welding, GTAW, SEM

Joints of dissimilar metals are commonly used in different industries such as power generation, chemical, automotive, electronics and nuclear industries, to combine different properties of these materials in a single component. More recently, welding technologies have been successfully used to manufacture hybrid microsystems consisting of different materials [1–3]. The weldability of dissimilar metals is determined by their atomic diameter, crystal structure and compositional solubility in the liquid and solid states. Diffusion in the weld pool often results in the formation of intermetallic phases, the majority of which are hard and brittle and are thus detrimental to the mechanical strength and ductility of the joint. Diffusion of alloying elements in the weld pool often leads to the formation of intermetallic phases. Many of these phases are hard and brittle and have detrimental effects on the mechanical strength, ductility and thermal and electrical conductivity of the joint [4].

Stainless steels are commonly used in welded joint section. Austenitic stainless steels (e.g. 316L and 304) represent more than 2/3 of the total stainless steel production. These stainless steels are preferred more than other stainless steel types due to their good weldability. Copper and copper alloys are one of the most versatile engineering materials. The combination of copper properties such as strength, conductivity, corrosion resistance, machinability and ductility make copper suitable for a wide range of applications.

Stainless steels have low thermal conductivity in comparison to copper and its alloys. When these alloys are used at high temperatures, heat dissipation to the environment is low because of their low thermal conductivity. Joining of copper to stainless steels can increase the heat dissipation from these alloys during high temperature applications and decrease the formation probability of intermetallic phases such as sigma phase after prolong heating, but high thermal conductivity of copper is one of the main limitations regarding to its welding. In other words, high thermal conductivity of copper tends to rapidly dissipate heat away from the weld zone,

leading to difficulties in reaching the melting temperature [5].

Elements of the welding arc physics

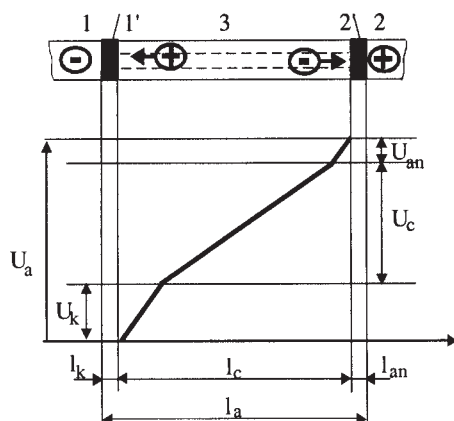
A welding arc is an electric discharge that develops primarily due to flow of current from cathode to anode. Flow of current through the gap between electrode and work piece needs column of charged particles for having reasonably good electrical conductivity.

These charged particles are generated by various mechanisms such as thermal emission, field emission secondary emission etc. Density of charged particles in gap governs the electrical conductivity of gaseous column. In an electric arc, electrons released from cathode (due to electric field or thermo-ionic emission) are accelerated towards the anode because of potential difference between work piece and electrode [6].

The cathodes used in GTAW are made of refractory material. A typical example of refractory cathode is a tungsten cathode; its melting point is $T_m = 3410^\circ\text{C}$, and its boiling point $T_b = 5660^\circ\text{C}$. Refractory materials can sustain high temperature without strong melting or vaporization. Vaporization is thus assumed to be negligible. For refractory material, thermo-field emission is the dominant emission process. Thermo-field emission is thermionic emission enhanced by the lowering of the surface potential barrier due to the presence of a space charge layer [7].

The direction the electrons flow towards is referred to as polarity. Electrons generally flow from a negatively charged (polarized) body to a positively charged body. Direct current electrode negative (DC-) is when a direct current power supply is used and the work piece is connected to the positive terminal. On the other hand, if the base material is connected to the negative terminal of a direct power supply then we are talking about direct current electrode positive (DC+) [8]. Moreover, about 70% of the heat in DC- polarity is directed to the work piece and 30% of the heat is directed to the electrode and vice versa when DC+ polarity is used. The difference in heat

* email: virlan_oana@yahoo.co.uk



1 – cathode;
1' – cathode region;
2 – anode;
2' – anode region;
 l_a – arc length;
 U_k – arc drop on the cathode region;
 U_c – arc drop on the arc column;
 U_{an} – arc drop on the anode region;
 l_k – length of cathode region;
 l_{an} – length of anode region;
 l_c – length of arc column.

Fig. 1. Regions of the electric arc

distribution leads to variations of the weld geometry. [9, 10, 11].

The electric arc has a quasi-stationary status, characterized by the following parameters: welding current intensity, I_s , anode voltage of the arc, U_a , pressure, p , temperature, T , and arc length, L_a .

There are three regions along the arc length: cathode region, k, anode region, A, and arc column, C (fig. 1).

The temperature emission of electrons depends on the nature of the metal and on the condition of the metal surface. The electron emission of the cathode is supported by the microscopic peaks of the superficial asperities, by certain faces of the metallic crystal and by certain surface impurities, which determines important current variations between various adjacent regions. The cathode region is continuously struck by a positive ion flow and the ions produce a micro-sandblasting effect of the liquid cathode. The value of the anode voltage is influenced neither by the welding current I_s nor by the composition of the gases in the arc. The temperature values of the anode region are higher than the temperature values of the cathode region [9].

Experimental part

For realizing the welded copper and stainless steel components we used such dimensions shown in Figure 2. The welding process used was the GTAW process, which offers a concentrated energy in place of welded joint and provides a very good quality of the obtained weld seam.

For the experimental part it was used an inverter based welding power source (CaddyTIG 2200i-ESAB). The polarities used in this experimental procedure were direct current negative polarity (DC-). The values of the main TIG welding parameters were: welding current intensity $I_s = 100A$ and arc voltage $U = 12-14V$.

The chemical composition of the materials used is presented in table 1 and their thermo-physic properties are presented in table 2.

As a result of the welded fitting we searched in keeping the thermo-physic properties of the materials in the area

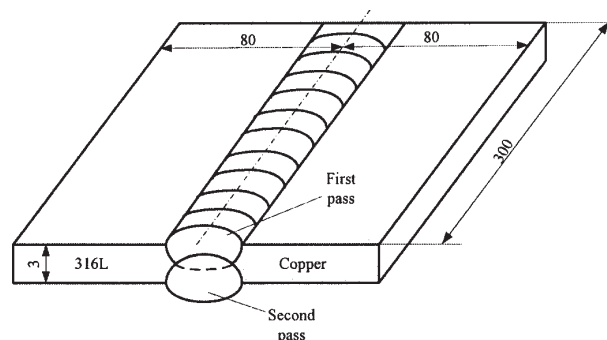


Fig. 2. Schematic illustration of joint design

of welded as well as achieving a homogeneous area in the weld.

In order to check the quality of the welded fitting obtained we have used methods of analysis of optical micrographic, electronic (SEM) and energy dispersive x-ray microanalysis (EDAX).

Results and discussions

After we obtained the samples, they were subject to non-destructive testing by using the visual method and the penetrating liquid method. No non-conformities resulted following the test.

After the welding process, in order to perform the metallographic analysis the samples were cut using a special cutting system at low cutting speeds with continuous cooling so as to prevent the analyzed zone from being affected by the heat. After the cutting process, the samples were cleaned from impurities and subject to a polishing process using metallographic paper with different granulations; finally, the samples were subject to polishing with abrasive diamond paste. The obtained metallographic structures are presented in figure 3.

Analyzing the micrographic images obtained from combining the welded joint that has achieved a uniform dispersion of the material in the matrix of the basis thereof.

In figure 4, SEM images are shown of the material of the weld.

Material	C [%]	Mn [%]	Si [%]	P [%]	S [%]	Cr [%]	Ni [%]	Mo [%]	Cu [%]	Fe [%]
316L	0.03	2.00	0.75	≤0.045	≤0.015	16.50-18.50	10.00-14.00	2.00-3.50	-	Bal.
Cooper	-	-	-	≤0.001	≤0.002	-	≤0.002	-	≥99.99	≤0.002
Cooper filler	-	-	-	≤0.001	≤0.002	-	≤0.002	-	≥99.99	≤0.002

Table 1
CHEMICAL COMPOSITION OF
BASE MATERIAL AND FILLER
MATERIAL

Material	Melting point (°C)	Boiling point (°C)	Density (g/cm ³)	Conductivity (W/m °C)	Heat capacity (J/(g °C))	Absorptivity (%)
316L	1400	2860	7.87	2.78	0.456	40
Cooper	1084	2562	8.96	3.97	0.386	3

Table 2
THERMOPHYSICAL PROPERTIES OF
MATERIALS AT ROOM TEMPERATURE

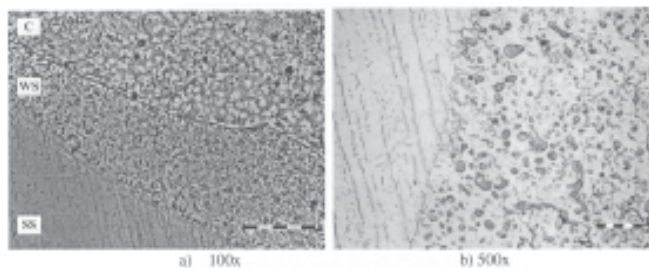


Fig. 3. Microscopic images obtained in the welded joints:
a) – magnification of 100x; b) - magnification of 500x, C – copper
base material, WS – welding seam, SS – stainless steel base
material

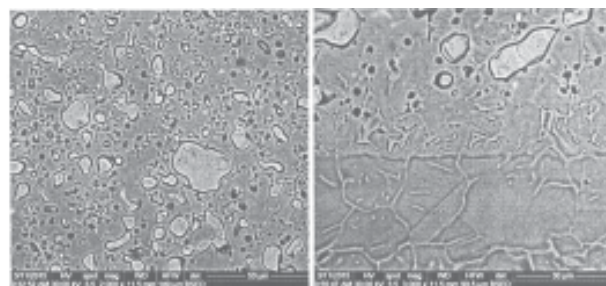


Fig. 4. SEM images with a) magnification of 2000x and b) detail of
the same sample with a magnification of 3000x

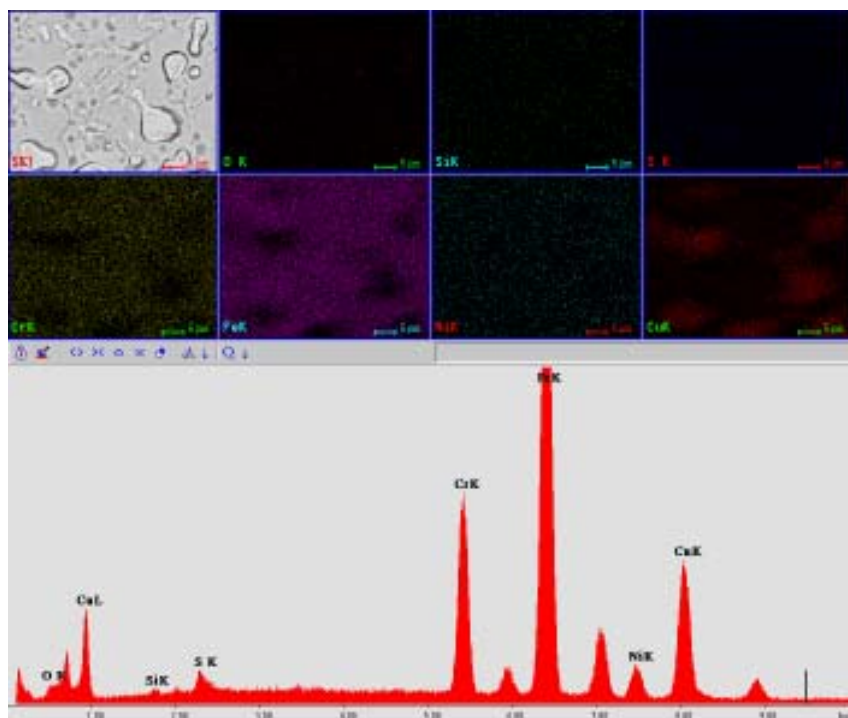
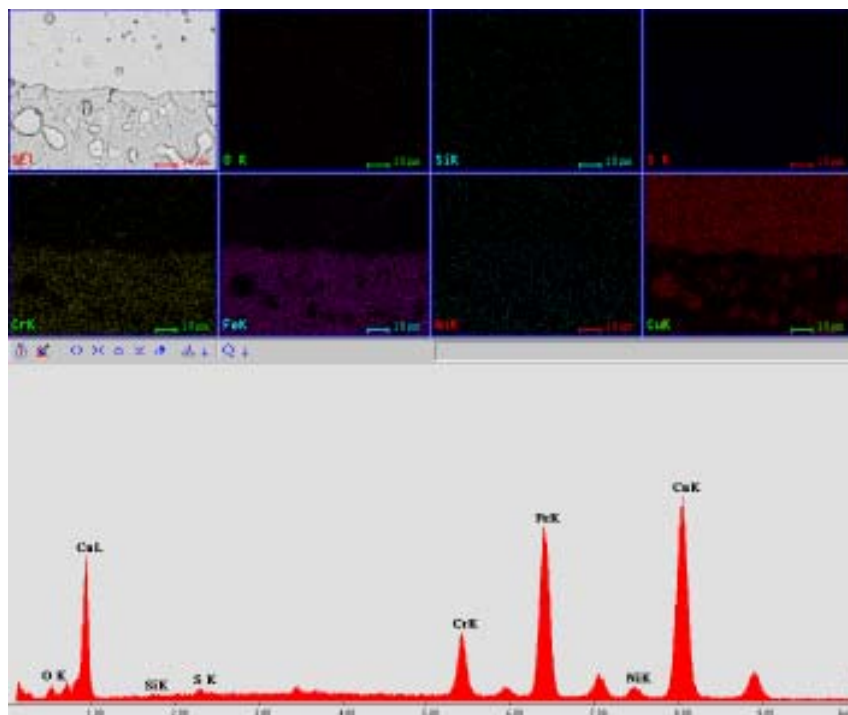


Fig. 5. The energy dispersive x-ray spectra of
the welding seam: a) - the weld area; b) - the
crossing area of the stainless steel

In the analysis of the image presented in figure 4, pictures taken at 2000x or 3000x time's multiplier, we noted that there is a good adhesion to the level of the crossing layers of materials and the weld material. The transition from basic materials to the welded seam was made through

the diffusion material in the filler material, making a good mix at the micro-structural level.

In order to obtain the local chemical composition of the samples the energy dispersive x-ray microanalysis (EDAX) was performed. The present spectrum in figure 5 shows

the chemical composition of the material in the weld and the crossing of the welding material and the stainless steel.

From the analysis shown in figure 5, we noted that in weld area we find a greater quantity of copper compared to the component elements of the stainless steel (Cr, Ni and Fe), a fact reflected in the filler material which was copper ramrod type. In the area of passing towards the stainless steel is a narrow area of copper diffusion of the filler material in the base material. This increases the conditions fulfilling required for the functioning of the conductivity of the welded joints.

Conclusions

The examination methods used provide important information on the quality of welded joints obtained.

The optical microscopic and electronic methods have shown that in the welded joints have not appeared non-conformities that lead to rejection of the sample.

Using x-ray spectroscopy method with energy dispersion provides us with information on the content of alloying elements in the welded joint area, elements that, depending on the percentage, influence the thermo-physic properties of the welded joints.

By using an appropriate welding technology and welding processes with concentrated energy source (e.g. GTAW); you can get good quality among the welded joints components with different thermo-physic properties. This is validated by the results of the performed examinations..

Acknowledgement: The work has been funded by the Sectoral Operational Programme Human Resources Development 2007-2013 of the Ministry of European Funds through the Financial Agreement POSDRU/159/1.5/S/134398.

References

1. A.M. OLOWINSKY, T. KRAMER, F. DURAND, SPIE Proc. Photon Process, Microelectron. Photonics 4637 (2002) 571–580.
2. Z. SUN, J.C. ION, J. Mater. Sci. 30 (1995) 4205–4214.
3. T.A. MAI, A.C. SPOWAGE, Characterisation of dissimilar joints in laser welding of steel–kovar, copper–steel and copper–aluminium, Materials Science and Engineering A 374 (2004) 224–233
4. S. G. SHIRI, M. NAZARZADEH, M. SHARIFITABAR, M.I S. AFARANI, Gas tungsten arc welding of CP-copper to 304 stainless steel using different filler materials, Trans. Nonferrous Met. Soc. China 22(2012) 2937–2942
5. I.MAGNABOSCO, P.FERRO, F. BONOLLO, L.ARNBERG, An investigation of fusion zone microstructures in electron beam welding of copper–stainless steel [J]. Materials Science and Engineering A, 2006, 424: 163–173.
6. *** Information on: <http://nptel.ac.in>, accessed on 12.03.2015
7. A. J. SHIRVAN, Modelling of Electric Arc Welding: arc-electrode coupling, Thesis for the degree of licentiate of engineering, Gothenburg, Sweden 2013
8. GH.SOLOMON, D.T.CICIC, Teoria proceselor de sudare (Theory of welding processes), Editura Bren, Bucharest, 2009
9. D. Dehelean, Sudarea prin topire (Fusion welding), Editura Sudura, Timișoara, 1997
10. GH.ZGURA, G.IACOBESCU, C.RONTESCU, D.T. CICIC, Tehnologie sudarii prin topire (Fusion welding technology), Editura Politehnica Press, Bucharest, 2007
11. R.M.A. HAMZA, A. ALORAIE, E. A. AL-FARAJ, Investigation effect of welding polarity in joint bead geometry and mechanical properties of shielded metal arc welding process, Journal of Engineering and Technology, Volume , Issue 3, 2011, 100-111
12. RADU, G. L., POPESCU, A.M., NICULAE, C. G. , RADUCANU, A. E., ONISEI, I., Identification by Liquid Chromatography-Mass Spectrometry of Herbal Food Supplements Adulterated with PDE-5 Inhibitors, Rev. Chim.(Bucharest), **66**, no. 1, 2015, p. 1

Manuscript received: 30.06.2015